Proceedings of the Sixth International Conference on
Railway Technology: Research, Development and Maintenance
Edited by: J. Pombo
Civil-Comp Conferences, Volume 7, Paper 3.6
Civil-Comp Press, Edinburgh, United Kingdom, 2024
ISSN: 2753-3239, doi: 10.4203/ccc.7.3.6

Evaluation Method of Railway Vehicles' Resistance Against a Tornado-like Vortex

Y. Nagumo and Y. Misu

**Research and Development Center of JR East Group,
East Japan Railway Company
Tokyo, Japan**

Abstract

In this study, the effects of tornado-like vortex parameters on the dynamic responses of a vehicle were evaluated using a dynamic analysis model, and a method for evaluation of the vehicles' resistance to overturning due to tornadoes was examined. Firstly, the model of wind speed field around a vortex was modified to reproduce all situations where a vehicle encounters a tornado-like vortex, and the dynamic analysis model for aerodynamic forces and vehicle responses was constructed. Secondly, using the constructed dynamic analysis model, the vehicle responses were evaluated by varying the vortex parameters to identify the conditions under which the responses became large. Finally, the dynamic analysis results under the identified conditions were compared with the quasi-static analysis results using the RTRI's detailed equation which used in the actual train operation. The results derived utilizing the constructed dynamic analysis model under the identified conditions showed that the RTRI's detailed equation could be used to evaluate vehicles' resistance to overturning on the safe side.

Keywords: gust, crosswind, critical wind speed of overturning, multi-body dynamics, RTRI's detailed equation, wheel load reduction rate.

1 Introduction

The safety of railway vehicles against crosswinds is ensured when the vehicles' resistance to overturning exceeds the external forces generated by the wind. To

quantitatively evaluate this condition, evaluation methods of the vehicles' resistance to overturning and of the external forces due to winds have been studied ([1]-[4]).

One of the external force evaluation methods is to constantly monitor winds with anemometers installed at one location (or several locations in some cases) within a pre-determined several-kilometer operation control section. Train operation is restricted when observed wind speeds exceed criteria, and the restriction is lifted when the wind speed decreases and remains below the criteria for a certain period of time. This method assumes that strong winds are continuous for several kilometers along the length of the operation control section, and that the wind speeds within the operation control section can be represented at the location where the anemometers are installed [1]. In addition, the time set for the lifting of the restrictions suggests that the high winds are assumed to continue for a certain period. Therefore, this external force evaluation method assumes spatially and temporally continuous strong winds, i.e., winds that can be regarded as steady flow. Based on this assumption in Japan, the Kunieda equation [2] and the RTRI's detailed equation[3], [4], which are applied in static or quasi-static analysis, are widely used as methods for evaluating the railway vehicles' resistance to overturning against steady flow.

Fixed anemometers placed every few kilometers, however, have a limited ability to capture locally occurring weather phenomena such as tornadoes. In response to a train overturn accident caused by a tornado in 2005 on Uetsu Main Line in Japan [5], Suzuki et al. [6] developed and introduced a new regulation method of train operation against gusts using Doppler radar. This method uses Doppler radar to detect and track tornado-like vortices and predict their maximum wind speeds and paths. If the maximum wind speed exceeds a predetermined criterion, train operations are suspended in sections where the detected vortices are predicted to reach. This method makes it possible to evaluate the external forces due to tornado-like vortices as the maximum wind speed. On the other hand, there is still room in evaluating the vehicles' resistance to overturning due to the tornado-like vortex, which are different from steady flow.

One of the differences between a tornado-like vortex and a steady flow is whether the wind speed changes rapidly in space and time. It has been pointed out by Hibino et al. [7] that when winds with rapidly changing speeds act on a vehicle, the vehicle responses could exceed that of a steady flow at a wind speed equal to its maximum. Therefore, a dynamic analysis model that can consider the characteristics of the tornado-like vortex, in which wind speeds change rapidly, is necessary to evaluate the influence of the tornado-like vortex on the vehicle responses. Baker and Sterling [8] proposed a conceptual design framework for loads on a structure, taking into account the relative position of the structure in relation to a moving tornado. However, they did not focus on a vehicle that travels and has dynamic responses. Zhang and Ishihara [9] proposed an analytical model to predict the dynamic responses of a vehicle to a tornado-like vortex using multi-body dynamics. However, this model assumed a wind speed field in which the tangential winds of the vortex were distributed along the direction of travel of the tornado-like vortex. In practice, the wind speed field around

the vortex varies in a complex manner depending on the direction and speed of the vortex travel, and the wind direction and speed of the tangential wind of the vortex. To reproduce all situations in which a vehicle encounters a tornado-like vortex, it is necessary to modify the wind speed field model to allow arbitrary relative positions and relative motions of the vortex and the vehicle. Using this modified and validated model of the wind speed field, a systematic parameter study should be conducted with vortex parameters as variables. Furthermore, in practical railway operations, a simpler model is required that can encompass the dynamic effects of the tornado-like vortex on the vehicle responses.

In this study, the effects of tornado-like vortex parameters on the dynamic responses of a vehicle were evaluated using a dynamic analysis model, and a method for evaluation of the vehicles' resistance to overturning due to tornadoes was examined. Firstly, the model of wind speed field around a vortex was modified to reproduce all situations where a vehicle encounters a tornado-like vortex, and the dynamic analysis model for aerodynamic forces and vehicle responses was constructed. Secondly, using the constructed dynamic analysis model, the vehicle responses were evaluated by varying the vortex parameters to identify the conditions under which the responses became large. Finally, the dynamic analysis results under the identified conditions were compared with the quasi-static analysis results using the RTRI's detailed equation which used in the actual train operation.

2 Dynamic Analysis Model Construction

2.1 Modification of Wind Speed Field Model

The existing model of wind speed field [9] assumed a situation where the tangential wind of vortex was distributed along the direction of vortex travel. Thus, the existing model could not represent situations where the direction of vortex travel and the tangential wind were different, or where the relative positions of the vortex and the vehicle were different. Therefore, in this study, the wind speed field model is modified to accurately reproduce situations in which a vehicle encounters a tornado-like vortex, considering arbitrary relative positions and motions of those.

Figure 1 shows the wind speeds and directions at the center of the vehicle when the vehicle encounters a vortex. Descriptions of the parameters are provided below the figure. V_a, ψ_a, V_r, ψ_r, and ψ_t are obtained using equations from (1) to (5), respectively.

$$V_\mathrm{a} = \sqrt{(V_\mathrm{r}\sin\psi_\mathrm{r} + V_\mathrm{t}\sin\psi_\mathrm{t})^2 + (V_\mathrm{r}\cos\psi_\mathrm{r} + V_\mathrm{t}\cos\psi_\mathrm{t})^2} \tag{1}$$

$$\psi_\mathrm{a} = \arctan\frac{V_\mathrm{r}\sin\psi_\mathrm{r} + V_\mathrm{t}\sin\psi_\mathrm{t}}{V_\mathrm{r}\cos\psi_\mathrm{r} + V_\mathrm{t}\cos\psi_\mathrm{t}} \tag{2}$$

$$V_{\mathrm{r}} = \sqrt{(V_{\mathrm{m}} \sin\psi)^2 + (V_{\mathrm{m}} \cos\psi + V_{\mathrm{v}})^2} \tag{3}$$

$$\psi_{\mathrm{r}} = \arctan\frac{V_{\mathrm{m}} \sin\psi}{V_{\mathrm{m}} \cos\psi + V_{\mathrm{v}}} \tag{4}$$

$$\psi_{\mathrm{t}} = \arctan\frac{x}{y} + \psi_{\mathrm{r}} \tag{5}$$

By formulating the wind speed field as described above, the relative position and relative motion of the vortex and the vehicle can be set arbitrarily.

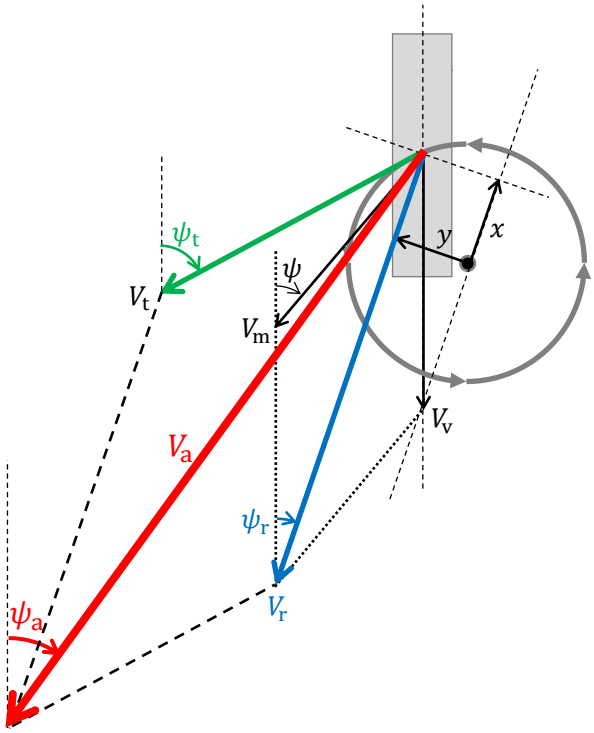

V_{t} : tangential wind speed of vortex
V_{m} : travel speed of vortex
V_{v} : relative wind speed generated by vehicle travel (Vehicle running speed)
V_{r} : relative wind speed composed of V_{m} and V_{v}
V_{a} : relative wind speed composed of V_{t} and V_{r}
ψ : relative angle between the direction of vortex travel and of vehicle travel
ψ_{t} : relative angle between the direction of tangential wind of vortex and of vehicle travel
ψ_{r} : relative angle between the direction of V_{r} and of vehicle travel
ψ_{a} : relative angle between the direction of V_{a} and of vehicle travel
x : distance parallel to the relative velocity V_{r} from vortex center to vehicle center
y : distance perpendicular to relative velocity V_{r} from vortex center to vehicle center

Figure 1: Wind speeds and directions at the center of vehicle when a vehicle encounters a vortex.

2.2 Aerodynamic Force Model

Aerodynamic forces acting on the vehicle are calculated based on the previous study [9]. Using the wind speeds and directions derived in the previous section, the aerodynamic forces acting on small areas of a vehicle are integrated over the vehicle body area to obtain the aerodynamic forces acting on the entire vehicle. It is assumed that the time series variation of aerodynamic forces follows the time series variation of wind speeds without delay. The aerodynamic forces, lateral force F_{S}, lift force F_{L}, and rolling moment M_{R}, are obtained by equations (6), (7), and (8), respectively.

$$F_{\mathrm{S}}(t) = \frac{1}{2}\rho H \int_{-2/L}^{2/L} V_a^2(x,t) \cdot C_{\mathrm{S}}\big(\psi_a(x,t)\big)dx \tag{6}$$

$$F_{\mathrm{L}}(t) = \frac{1}{2}\rho H \int_{-2/L}^{2/L} V_a^2(x,t) \cdot C_{\mathrm{L}}\big(\psi_a(x,t)\big)dx \tag{7}$$

$$M_{\mathrm{R}}(t) = \frac{1}{2}\rho H^2 \int_{-2/L}^{2/L} V_a^2(x,t) \cdot C_{\mathrm{M}}\big(\psi_a(x,t)\big)dx, \tag{8}$$

where ρ is air density, H is body height, L is body length, C_{S} is the coefficient of lateral force, C_{L} is the coefficient of lift force, and C_{M} is the coefficient of rolling moment around the car body center.

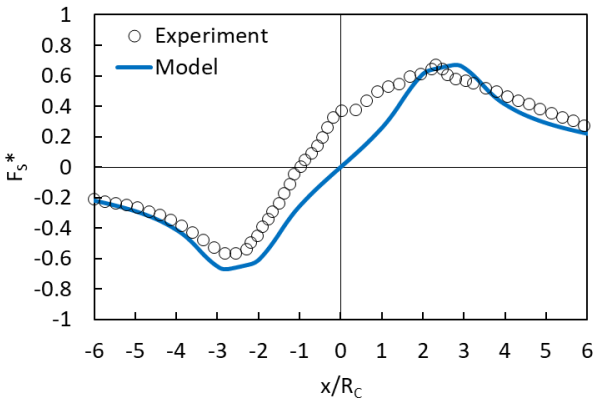

Figure 2: Comparison of side forces obtained experimentally and estimated by the constructed model

Figure 2 compares the side forces, which contribute most to vehicle overturning, between those obtained experimentally [10] and those estimated by the analytical model. The analytical model uses aerodynamic coefficients obtained from wind tunnel tests with steady flow using a vehicle model with the same body geometry as in the experiment. Side forces shown in Figure 2 are made dimensionless using Equation (9). It shows that the maximum values of both are in good agreement.

$$F_S^* = \frac{F_S}{0.5\rho \cdot max[V_t]^2 \cdot S_A} \tag{9}$$

where V_t, S_A are the tangential wind speed of the vortex and the lateral area of the vehicle, respectively.

2.3 Vehicle model

Based on the previous study [9], a vehicle model with multi-body dynamics is developed. Figure 3 shows an image of the vehicle model. The program used is the commercial software Simpack2017. A vehicle consists of 7elements: 1 body, 2 bogies, and 4 wheelsets, and each element has 6 degrees of freedom, creating a single vehicle model with 42 degrees of freedom in total. The parameters considered in the vehicle model are the same in the RTRI's detailed equation. Each element of the vehicle is connected by springs and dampers.

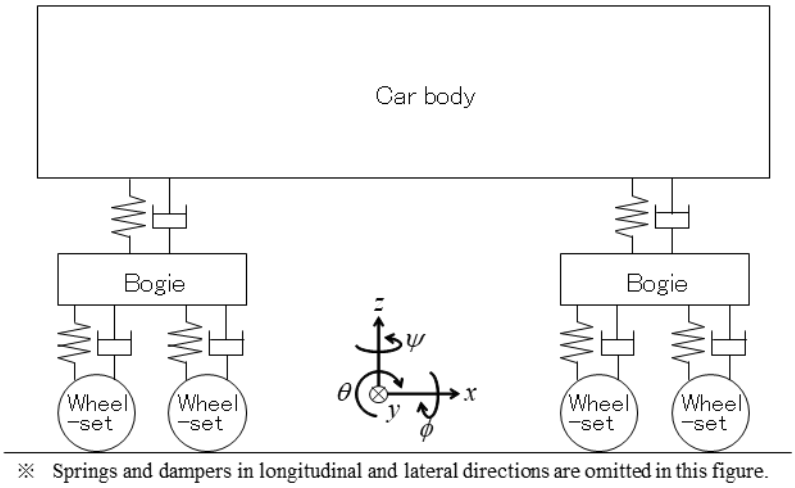

Figure 3: An image of vehicle model

3 Parameter Study

3.1 Evaluation Indicators and Conditions

Parameter studies are conducted using the analytical model constructed in the previous section to identify the conditions under which the vehicle responses become large. The evaluation indicators for vehicle responses are maximum wheel load reduction rate $D_{\max}$ and Dynamic Amplification Factor (DAF). The maximum wheel load reduction rate $D_{\max}$ is the maximum value of the time-series change in wheel load reduction rate due to the tornado-like vortex and is expressed by equation (10).

$$D_{\max} = 1 - \min[P_{\mathrm{w}}] / P_0, \tag{10}$$

where $\min[P_{\mathrm{w}}]$ is the minimum value of windward side wheel load P_{w}, and P_0 is static wheel load. A larger $D_{\max}$ indicates a larger vehicle response. DAF is the value obtained by dividing $D_{\max}$ by the wheel load reduction rate due to steady flow, D_{S}, as shown in Equation (11).

$$DAF = D_{\max}/D_{\mathrm{S}}, \tag{11}$$

A larger DAF indicates that the dynamic amplification effects of the tornado-like vortex on the vehicle response is greater.

The vehicle is assumed to be a lead car of a commuter train, and the surrounding structure is assumed to be flat ground. The aerodynamic force coefficients of the vehicle on the flat ground are obtained by wind tunnel tests using the scaled models and structures ([11], [12], [13]) and corrected by the method of Moriyama et al. [14]. The vortex parameters to be varied are the seven items shown in Figure 4. The maximum tangential wind speed, $\max[V_{\mathrm{t}}]$, of the vortex is varied by the parameter $V_{\max}(=\max[V_{\mathrm{t}}]+V_{\mathrm{m}})$. Considering that the indicator for the train operation control against gusts using Doppler radar is the maximum wind speed $V_{\max}$, the travel speed of vortex V_{m} is accounted for in the parameter as the ratio of V_{m} to the maximum wind speed $V_{\max}$. Table 1 shows the ranges and basic values of each parameter. In this parameter study, one item is varied, and the others use basic values at a time.

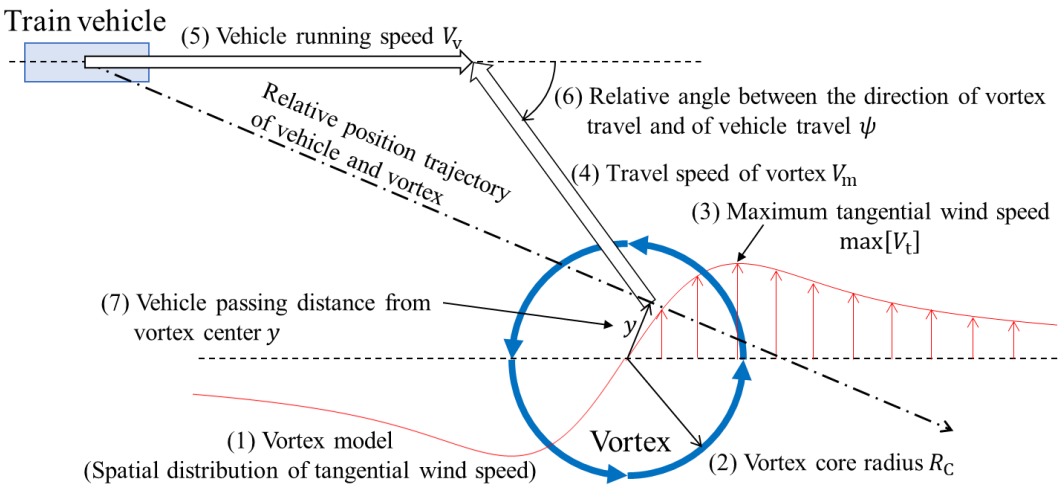

Figure 4: Vortex parameters considered in parameter studies

Parameter	Option / Range	Basic value
Vortex model	Rankine[15] Burgers-Rott[16], [17] Sullivan[18]	Burgers-Rott
R_{C} [m]	$10 \le R_{\mathrm{C}} \le 100$	20, 40, 80
$V_{\max}$ [m/s]	$15 \le V_{\max} \le 30$	30
V_{m} [m/s]	$0 \le V_{\mathrm{m}} \le V_{\max}$	$0.5V_{\max}$
V_{v} [km/h]	$0 \le V_{\mathrm{v}} \le 120$	120
ψ [deg]	$-90 \le \psi \le 90$	90
y [m]	$-R_{\mathrm{C}} \le y \le R_{\mathrm{C}}$	0

Table 1: Ranges and basic values of each parameter

3.2 Parameter Study Results

The effects of each parameter on vehicle responses are checked and the conditions under which the vehicle responses increase are identified. Figure 5 compares the effects of Rankine, Burgers-Rott, and Sullivan's vortex models on the vehicle response. Burgers-Rott model tends to maximize both $D_{\max}$ and DAF. This is because the Burgers-Rott model has less wind speed variation near the maximum wind speed, resulting in larger maximum calculated aerodynamic forces compared to other vortex models.

Figure 6 shows the effects of the vortex core radius, R_c, on the vehicle response. It shows that $D_{\max}$ and DAF are large when R_c is 20 – 30 m. If the vortex is too small, the time of exposure to the maximum aerodynamic force is shortened, and conversely, if the vortex is too large, the rise in wind speed is slowed and the dynamic amplification effect is reduced.

Figure 7 shows the effects of the maximum wind speed of the vortex, $V_{\max}$, on the vehicle response. Since the aerodynamic force increases as $V_{\max}$ increases, $D_{\max}$ also increases. This is the same trend as in the case of steady flow. On the other hand, DAF remains constant regardless of the maximum wind speed. This indicates that the dynamic amplification effect due to the tornado-like vortex is independent of the maximum wind speed within the wind speed range targeted by the railway field. So, $V_{\max}$ is set to 30 m/s as the identified value as in Table 2. Details will be explained in later section.

Figure 8 shows the effects of vortex travel speed, V_m, on vehicle response. V_m is evaluated by the coefficient $c_t (= V_m/V_{\max})$. $c_t = 0$ indicates that V_m is 0, i.e., the vortex is not moving and remains in one place. $c_t = 1$ indicates that V_m equals to $V_{\max}$, i.e., the vortex is not rotating. $D_{\max}$ is minimum when the coefficient c_t is around 0.6 and maximum when $c_t = 0$. DAF is minimum when $c_t = 1$ and increases with decreasing c_t. The condition where the tornado-like vortex has the greatest effect is $c_t = 0$; the vehicle response tends to be larger when the travel speed V_m is smaller. However, since $V_m = 0$, i.e., the tornado is stationary, is not realistic, c_t is set at 0.4 based on observations of winter tornadoes in Japan.

Figure 9 shows the effects of vehicle running speed, V_v, on vehicle response. As V_v increases, $D_{\max}$ and DAF tend to increase. This is due to the increase in aerodynamic forces caused by the larger relative wind speed and the increased dynamic amplification effect caused by the shorter rise time of the wind speed. Therefore, it is reasonable to assume the maximum running speed of the vehicle as the condition under which the vehicle responses increase.

Figure 10 shows the effects of the relative angle between the vortex and vehicle direction of travel ψ on the vehicle response. ψ is set to be positive for rightward and negative for leftward, with the direction of vehicle travel as 0. What differs from a steady flow condition is that the wheel load reduction occurs even when $\psi = 0$, and

that the magnitude of the vehicle responses differs depending on whether ψ is positive or negative even though the absolute value of ψ is the same. The former is because the tornado-like vortex has a rotating component, so a crosswind acts on the vehicle even if the relative angle is 0. The latter is because tornado-like vortices generally rotate counterclockwise in the Northern Hemisphere, so that the way the wind impacts the vehicle differs depending on whether ψ is positive or negative even when the absolute value of the relative angle is the same. $D_{\max}$ is greatest when the relative angle ψ is around 60 degrees. DAF reaches its maximum when ψ is near 0 degrees, at which point $D_{\max}$ is small. Under negative relative angle ψ conditions, both $D_{\max}$ and DAF are small.

Figure 11 shows the effects of the vehicle passing distance from the vortex center, y, on the vehicle response, nondimensionalized by the vortex center radius R_c. The distance y is positive when the vehicle passes through the left side of the vortex and negative when the vehicle passes through the right side of the vortex. Since the vortex has a counterclockwise direction of rotation, the magnitude of the vehicle responses differs for positive and negative y. $D_{\max}$ is maximum when y is around 0.6 times R_c, which indicates that the responses become large when the vehicle passes on the left side of the vortex. This is because the direction in which the vehicle and the vortex approach each other and the wind direction of the tangential wind speed of the vortex are opposite, resulting in higher relative wind speeds.

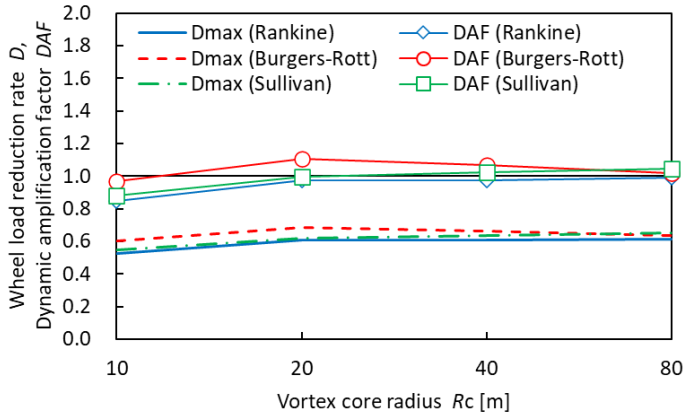

Figure 5: Effects of vortex model on vehicle response

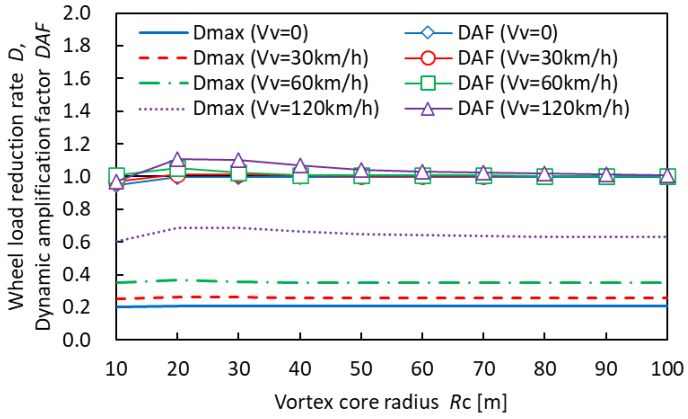

Figure 6: Effects of vortex core radius on vehicle response

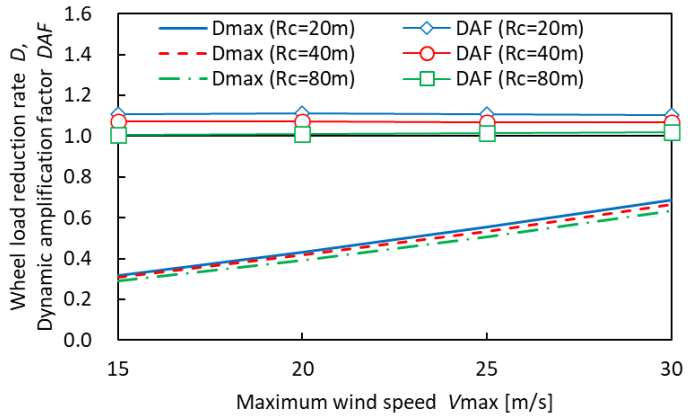

Figure 7: Effects of maximum wind speed of vortex on vehicle response

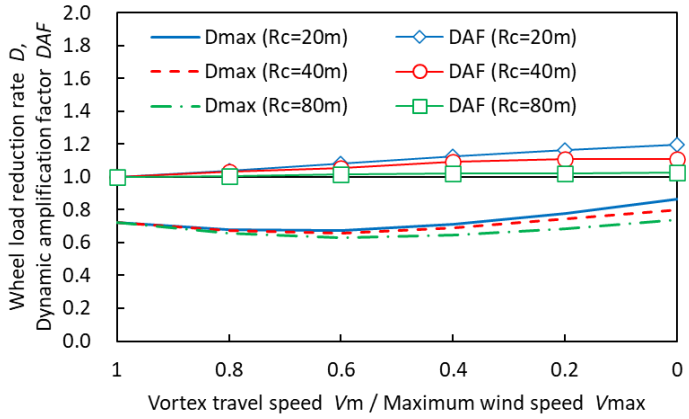

Figure 8: Effects of vortex travel speed on vehicle response

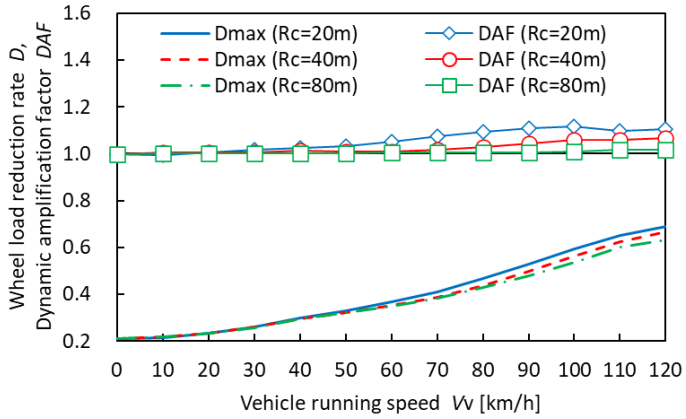

Figure 9: Effects of vehicle running speed on vehicle response

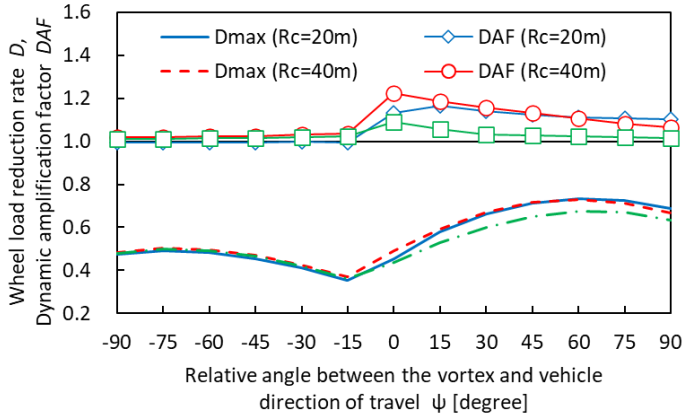

Figure 10: Effects of relative angle between vortex and vehicle direction of travel on vehicle response

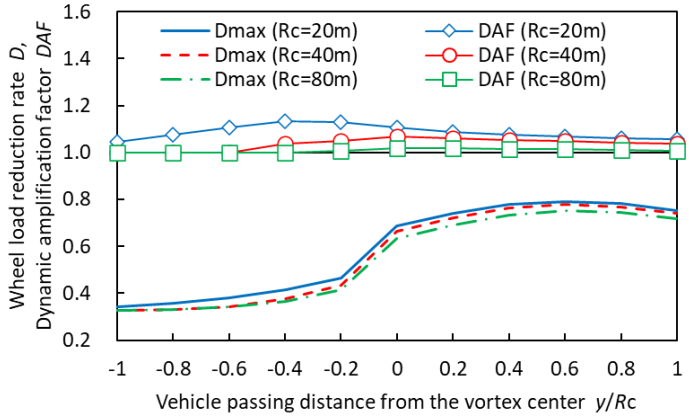

Figure 11: Effects of vehicle passing distance y from vortex center on vehicle response

The conditions for larger vehicle responses identified by the parameter study are shown in Table 2 as the identified values. Note that in Figures 5 to 11, the evaluations

were performed with the basic values shown in Table 1 for parameters other than the target parameters, in reality, however, some parameters interact with each other. Therefore, Table 2 shows the identified values with more detailed parameter adjustments.

Parameter	Identified value
Vortex model	Burgers-Rott
R_C [m]	30
V_{max} [m/s]	30
V_m [m/s]	0.4 V_{max}
V_v [km/h]	120
ψ [deg]	70
y [m]	0.5 R_C

Table 2: Identified values

4 Evaluation of Vehicle Response by the RTRI's detailed equation

By performing the dynamic analysis model constructed in section 2, it is possible to evaluate the vehicle responses, including the dynamic effects of the tornado-like vortex. On the other hand, in practical railway operations, it is expected that a simpler method to evaluate vehicles' resistance to overturning that can consider the effects of the tornado-like vortex. In this section, the applicability of the RTRI's detailed equation to the evaluation of the vehicles' response to overturning due to the tornado-like vortex is verified by comparing the results of the dynamic analysis model constructed in section 2 and the results of quasi-static analysis using the RTRI's detailed equation under the identified conditions in section 3.

Figure 12 shows the results of comparing the maximum wheel load reduction rate D_{max} obtained by the dynamic analysis model for the tornado-like vortex, the wheel load reduction rate D_{HBN} calculated by the RTRI's detailed equation assuming the steady flow, and the wheel load reduction rate D_S calculated by the dynamic analysis model assuming the steady flow. The identified values in Table 2 are used as the conditions of the tornado-like vortex, and V_{max} is set as the wind speed of the steady flow used in the calculation of D_{HBN} and D_S. Comparing D_{max} with D_S, the values are about the same when the vehicle running speed is low, but D_{max} becomes relatively large as the running speed increases. This is because the dynamic amplification factor DAF increases as the vehicle running speed increases. Comparing D_{HBN} and D_{max}, it can be seen that D_{HBN} is larger at any running speed than D_{max}. This is because the vehicle response is evaluated to be larger due to the safety margin included in the RTRI's detailed equation, and this margin encompass the dynamic amplification effects of the vehicle responses due to the tornado-like vortex. From the above, it can be said that although the wheel load reduction rate is greater in the tornado-like vortex than in steady flow, the RTRI's detailed equation can be used to safely evaluate the vehicle response to the tornado-like vortex.

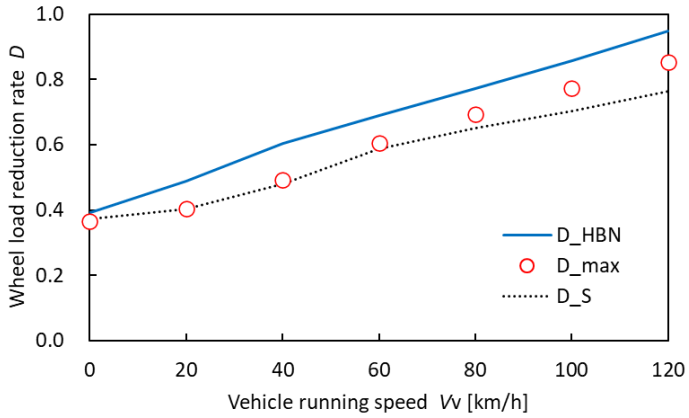

$D_{\max}$: maximum wheel load reduction rate obtained by the dynamic analysis model constructed in this study

D_{HBN}: wheel load reduction rate calculated by the RTRI's detailed equation assuming the steady flow

D_{S}: wheel load reduction rate calculated by the dynamic analysis model assuming the steady flow

Figure 12: Comparison of wheel load reduction rates, $D_{\max}$, D_{HBN}, and D_{S}

4 Conclusion

In this study, the effects of tornado-like vortex parameters on the dynamic responses of vehicles were evaluated by a dynamic analysis model. The conclusions obtained are as follows:

(1) The model of wind speed field around the vortex was modified to reproduce all situations where a vehicle encounters a tornado-like vortex, and the dynamic analysis model for aerodynamic forces and vehicle responses was constructed. This enables the evaluation of the vortex and vehicle with arbitrarily relative positions and motions.

(2) Using the constructed dynamic analysis model, the vehicle responses were evaluated by varying the vortex parameters. This clarified the trend and sensitivity of the parameters to the vehicle responses and identified the conditions under which the vehicle responses become large.

(3) The dynamic analysis results under the identified conditions were compared with the quasi-static analysis results by the RTRI's detailed equation. The comparisons showed that, although the vehicle responses due to the tornado-like vortex are larger than those due to the steady flow, it is possible to evaluate the vehicle resistances on the safe side using the RTRI's detailed equation.

References

[1] Y. Misu, T. Ishihara, "Prediction of frequency distribution of strong crosswind in a control section for train operations by using onsite measurement and

numerical simulation", Journal of Wind Engineering and Industrial Aerodynamics, 174: 69-79, 2018.
[2] M. Kunieda, "Theoretical study on the mechanics of overturn of railway rolling stock", Railway Technical Research Report, 793: 1-15, 1972. (in Japanese)
[3] Y. Hibino, H. Ishida, "Static Analysis on Railway Vehicle Overturning under Crosswind", RTRI Report Vol. 17, No. 4, 39–44, 2003. (In Japanese)
[4] Y. Hibino, Y. Misu, T. Kurihara, A. Moriyama, M. Shimamura, "Study of new methods for train operation control in strong winds", JR East Technical Review, 19, 31-36, 2011.
[5] Aircraft and Railway Accidents Investigation Commission, "Railway Accident and Incident Report", No. RA2008–4, 2008, (In Japanese)
[6] H. Suzuki, K. Kusunoki, C. Fujiwara, H. Inoue, "Development of train operation control method against wind gusts using doppler radar". Proceedings of the 15th International conference on wind engineering (ICWE15), A182113,2019.
[7] Y. Hibino, H. Kanemoto, Y. Sakuma, "A study on vehicle response to a sudden gust of wind". Transactions of the Japan Society of Mechanical Engineers, Series C, 2013, 79.806: 3410-3419.
[8] C. J. Baker, M. Sterling, "A conceptual model for wind and debris impact loading of structures due to tornadoes", Journal of Wind Engineering and Industrial Aerodynamics, Vol.175, 283-291, 2018.
[9] D. Zhang, T. Ishihara, "Numerical study of tornado-induced unsteady crosswind response of railway vehicle using multibody dynamic simulations", Journal of Wind Engineering and Industrial Aerodynamics, Vol.222, 104919, 2022.
[10] M. Suzuki, N. Okura, "Study of aerodynamic forces acting on a train using a tornado simulator", Mechanical Engineering Letters, 2016, 2: 16-00505-16-00505.
[11] M. Suzuki, K. Tanemoto, T. Maeda, "Aerodynamic characteristics of train/vehicles under crosswinds". Journal of Wind Engineering and Industrial Aerodynamics, 91(1), 209–218, 2003.
[12] M. Suzuki, Y. Hibino, "Field tests and wind tunnel tests on aerodynamic characteristics of train/vehicles under crosswind". Quarterly Report of RTRI 57(1), 55–60, 2016.
[13] K. Tanemoto, M. Suzuki, H. Saito, A. Ido, "Results of wind tunnel tests for aerodynamic coefficients of railway vehicles", RTRI report, 27(1), 47-50, 2013. (In Japanese)
[14] A. Moriyama, K. Horioka, K. Doi, "Device and method for calculating wind velocity", JP2013-086722, IPC: B61K 13/00 (2006.01)
[15] W. J. M. Rankine, "A Manual of Applied Physics", 10th ed., Charles Griff and Co, 1882.
[16] J. M. Burgers, "A mathematical model illustrating the theory of turbulence", Advances in Applied Mechanics, Vol.1, p.171-199, 1948.
[17] N. Rott, "On the viscous core of a line vortex", Zeitschrift für Angewandte Mathematik und Physik, Vol.9, No.5-6, p.543-553, 1958.
[18] R. D. Sullivan, "A two-cell vortex solution of the Navier-Stokes equations", Journal of the Aerospace Sciences, Vol.26, No.11, p.767-768, 1959.